

# Anisotropic Distributions of Ion Fragments Produced by Dissociative Ionization of Halogenated Ethylenes in Intense Laser Fields

Marta Castillejo,\* Margarita Martín, and Rebeca de Nalda

*Instituto de Química Física “Rocasolano”, CSIC, Serrano 119, 28006 Madrid, Spain*

Stelios Couris† and Emmanuel Koudoumas

*Foundation for Research and Technology–Hellas, Institute of Electronic Structure and Laser, P.O. Box 1527, 711 10 Heraklion, Crete, Greece*

*Received: September 10, 2001; In Final Form: January 2, 2002*

The angular distributions of fragments arising from dissociative ionization of chloroethylene ( $\text{H}_2\text{C}=\text{CHCl}$ ), bromoethylene ( $\text{H}_2\text{C}=\text{CHBr}$ ), and 2-chloroethenylsilane ( $\text{H}_3\text{SiHC}=\text{CHCl}$ ) by a linearly polarized pulsed laser field (800 nm, 50 fs,  $2 \times 10^{14} \text{ W cm}^{-2}$ ) have been measured using a time-of-flight mass spectrometer. The angular distributions of the multiply charged halogen and silicon ions originating from different molecules are markedly anisotropic, yielding a maximum signal for a laser polarization along the axis of the time-of-flight detector. In contrast, the anisotropy of the distributions of the multiply charged carbon ions depends on the parent molecule: for chloroethylene and bromoethylene they are peaked preferentially in the direction parallel to the laser polarization, for 2-chloroethenylsilane they are peaked perpendicular to it. The anisotropy of all the above distributions is found to increase with the charge multiplicity of the ion fragment. The fragment anisotropies are discussed in terms of the molecular alignment, due to the nonresonant polarizability interaction, and of the selection of orientation in the ionization and dissociation dynamics in the strong laser field.

## 1. Introduction

Recent studies of the interaction of intense laser fields with organic molecules explore a variety of its aspects, including ionization and fragmentation,<sup>1–4</sup> Coulomb explosion following multiple electron emission, spatial alignment of the molecular axis,<sup>5–9</sup> and high harmonic generation.<sup>10,11</sup> Molecular properties such as geometry, type of bonding, molecular size, polarizability, etc., have been shown to play a significant role in the laser–molecule interactions, despite the fact that at high laser intensities, above  $10^{13} \text{ W cm}^{-2}$ , the intramolecular Coulomb field is severely distorted and massive Stark shifts of the molecular energy levels are induced.

Studies of dissociative ionization of diatomic and polyatomic molecules have shown that laser polarization strongly affects the fragment angular emission patterns.<sup>6–8,12–17</sup> For diatomic and small polyatomic systems, channel-resolved and energy-resolved experiments<sup>8,14,18–20</sup> have provided a detailed picture of the mechanisms involved. However, for larger molecules the amount of dissociative channels is too large and more basic techniques have to be used to obtain information on the dissociative ionization process.<sup>2,6,7,21</sup> Anisotropies observed in the fragment angular distributions are now believed to arise from (a) alignment of the molecular axis which takes place via the interaction of the oscillating electric field of the laser with the molecular polarizability,<sup>22</sup> and (b) selection of orientation due to the angular dependence of the barrier to ionization.<sup>14–16</sup> Several groups have recently reported two-laser experiments where the first, nonresonant laser beam is used to align the molecules and the second resonant beam to probe such an

alignment.<sup>23–25</sup> The understanding of the relative roles of the above mechanisms is of considerable current interest, particularly in polyatomic systems.

Here we report a study of the laser-induced ionization and dissociation with laser pulses with a wavelength of 800 nm, a duration of 50 fs, and intensity up to  $2 \times 10^{14} \text{ W cm}^{-2}$ , of a set of organic molecules: chloroethylene ( $\text{H}_2\text{C}=\text{CHCl}$ ), bromoethylene ( $\text{H}_2\text{C}=\text{CHBr}$ ), and 2-chloroethenylsilane ( $\text{H}_3\text{SiHC}=\text{CHCl}$ ). The angular distributions of fragments arising from dissociative ionization of these compounds have been measured using time-of-flight (TOF) mass spectrometry. Due to the complexity of the molecules under study and the large number of reported dissociation channels,<sup>26–28</sup> detailed channel-resolved measurements (as reported for smaller molecular systems) are not feasible and we have measured here the dependence of the mass spectra with laser intensity and polarization angle of the linearly polarized laser. The choice of these molecules offers the opportunity of elucidating the role of the highly electronegative halide substituents and of the high polarizability of the C–halide bonds in the laser–molecule interaction. In all three molecules, the carbon–halogen bond is the most polarizable one. Chloro- and bromoethylene are planar systems, whereas in 2-chloroethenylsilane the Si–H bonds lie outside the molecular plane. For comparison, additional experiments were performed in cyclopropane, a cyclic alkane lacking the highly polarizable carbon–halogen bonds of the above systems. The effect of the angle between the laser electric field and the detection axis of the TOF on the angular distributions of the ions consist in a strong enhancement of the yield of multiply charged halogen and Si fragment ions for a laser polarization along the direction of the TOF detector. In contrast, the anisotropy of the distributions of the multiply charged carbon ions depends on the parent molecule: for chloroethylene and

\* Corresponding author. E-mail: marta.castillejo@iqfr.csic.es.

† Present address: ICEHT-FORTH, P.O. Box 1414, 26500 Patras, Greece.

bromoethylene they are peaked preferentially in the direction parallel to the laser polarization, for 2-chloroethylsilane they are peaked perpendicular to it. The anisotropy of all the above distributions has been found to increase with the charge multiplicity of the ion fragment. The fragment anisotropies are discussed in terms of the molecular alignment due to the nonresonant polarizability interaction and of the selection of orientation in the ionization and dissociation dynamics in the strong laser field.

## 2. Experimental Section

We measured the dependence of the photoionization and photofragmentation processes on laser intensity and polarization. The experimental setup was described previously,<sup>3,4</sup> and only a brief summary is given here.

The laser system is an amplified Ti:Sapphire laser delivering 50 fs pulses at 800 nm with a line width of about 40 nm. It consists of a Mira Ti:Sapphire oscillator (Coherent) and a BMI regenerative Ti:Sapphire amplifier (BMI). The oscillator, pumped by a Verdi (800 nm) diode laser (Coherent), delivers pulses of a 50 fs duration at a repetition rate of 76 MHz with 0.7 W power. The oscillator output is stretched and then used as seeding for the regenerative Ti:Sapphire amplifier (ALPHA 1000US), which is pumped by the second harmonic of a BMI Nd:YLF laser operating at 1 kHz. The amplified pulse is then compressed to get an output of 50 fs. The pulses are characterized using a homemade autocorrelator.

The linearly polarized laser beam at 800 nm was focused with a 15 cm lens at the center of the extraction region of a time-of-flight (TOF) mass spectrometer. The pulse energy could be continuously varied in the range of 8–500 mJ by means of Glan polarizers and was measured at the exit of the chamber with a power meter (Moletron J3-09). As measured in analogous systems,<sup>29</sup> no significant distortion of the pulse length or of the spectral characteristics of the laser due to the interaction with the optical elements that couple the laser beam into the interaction chamber was expected. To check for possible nonlinear effects caused by the Glan polarizers, we carried out additional measurements in which the laser intensity was controlled by means of variable neutral-density filters; no significant alterations of the mass spectra were thus found. The laser intensities were calibrated by measuring the saturation intensity for the ionization of Xe.<sup>30,31</sup> The range of intensities used in the present study was between  $3 \times 10^{12}$  and  $2 \times 10^{14}$  W cm<sup>-2</sup>. The polarization plane of the laser beam, defined by the Glan polarizer, could be rotated using a half-wave plate. The polar angle of a fragment was defined as the angle between the axis of the TOF detector and the polarization vector of the laser field. The laser field was polarized parallel to the TOF axis in the case of a p-polarization and perpendicular to it in s-polarization.<sup>7</sup>

The mass spectra were measured with a linear TOF spectrometer. The photoions generated in the ionization and fragmentation processes were accelerated between a repeller plate (+1900 V) and a grounded electrode 1.5 cm apart, passed into a 60 cm long TOF tube, and detected and amplified with a pair of microchannel plates (MCP) of a 2.54 cm diameter. The MCP signals were fed into a LeCroy 9414 digital oscilloscope, interfaced with a PC. The mass spectra were typically averaged over 200 laser shots.

Samples of the pure molecular compounds at stagnation pressures between 1300 and 5300 Pa were expanded into the vacuum chamber through a 0.3 mm pulsed nozzle (Laser Technics). The laser interaction zone is about 2 cm downstream

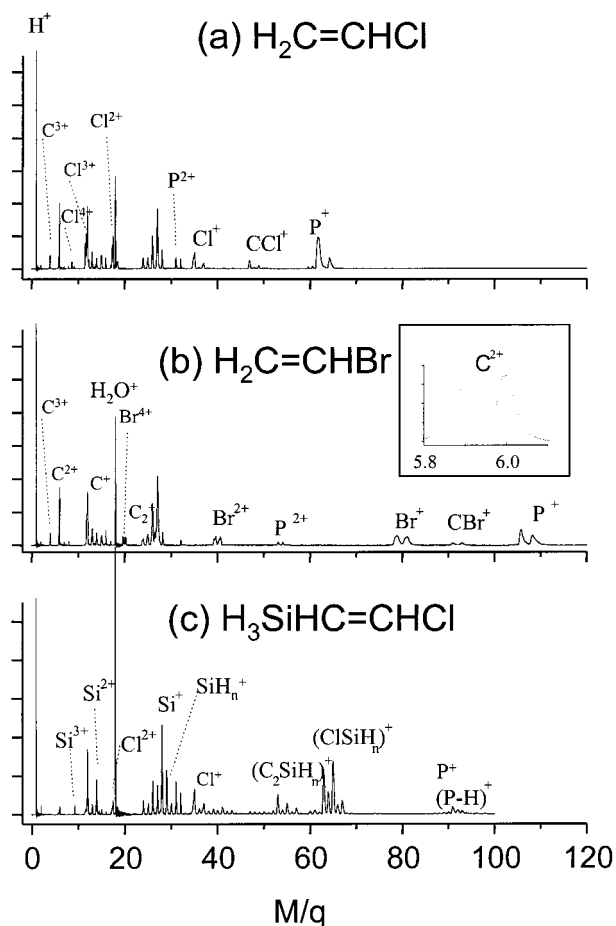


**Figure 1.** TOF spectra of (a) chloroethylene, (b) bromoethylene, and (c) 2-chloroethylsilane recorded, respectively, at laser intensities of  $1.85 \times 10^{14}$ ,  $1.9 \times 10^{14}$ , and  $5.1 \times 10^{13}$  W cm<sup>-2</sup>. The inset in (b) illustrates (for C<sup>2+</sup>) the typical double peak structure of the multiply charged ions observed in this work. The laser is p-polarized along the direction of the TOF detector. Parent molecular ions are labeled P<sup>+</sup>. The position of C<sup>2+</sup>, C<sup>+</sup>, H<sub>2</sub>O<sup>+</sup>, and C<sub>2</sub><sup>+</sup> ions is indicated in (b).

from the nozzle. The molecules are cooled to an estimated rotational temperature of about 50 K.

Chloroethylene and bromoethylene were purified by trap-to-trap distillation. 2-Chloroethylsilane was synthesized according to the method described in ref 32 as a 1:3 mixture of cis and trans isomers. These compounds were found by gas chromatography to be 95% pure. Cyclopropane (Linde) had a 95% purity rating.

## 3. Results

**3.1. Mass Spectra.** For each compound, we measured the TOF spectra at, typically, 16 different laser intensities ranging between  $3 \times 10^{12}$  and  $2 \times 10^{14}$  W cm<sup>-2</sup> for a p-polarization of the laser. These measurements made it possible to trace the dependence on the laser intensity of the parent and fragment ion signals and of the splitting observed for the multiply charged ions.

Figure 1 shows typical mass spectra of the three ethylene derivatives obtained at a laser intensity of about  $2 \times 10^{14}$  W cm<sup>-2</sup>. An extensive fragmentation is observed in all three cases, attesting to a great variety of fragmentation channels available for these molecules.<sup>26–28</sup> Despite the extensive dissociation, the singly and doubly ionized parent molecule intensities are not negligible, even at the highest laser power used in this work. Besides the parent ion, the mass spectra of chloro- and

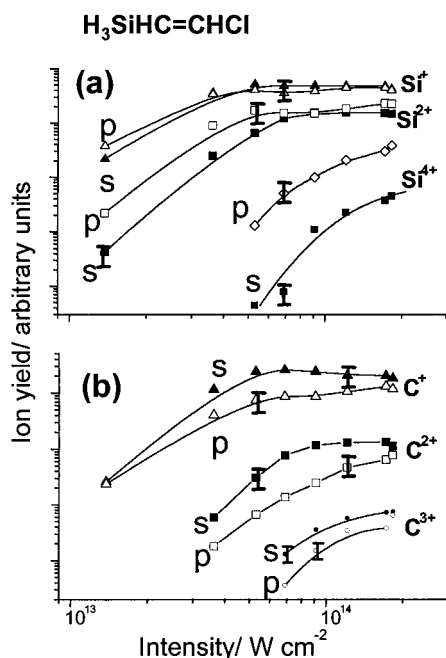


**Figure 2.** Dependence with laser intensity of (a) Si and (b) C ions resulting from the dissociative ionization of 2-chloroethylsilane. Full and open symbols are for s- and p- laser polarization, respectively. Typical error bars are indicated in each plot. Lines are drawn to guide the eye.

bromoethylene show the formation of halogen-containing diatomic ions,  $CX^+$  ( $X = Cl, Br$ ), carbon-containing fragments,  $CH_n^+$  ( $n = 1-3$ ) and  $C_2H_n^+$  ( $n = 0-3$ ), and of halogen, carbon, and hydrogen atomic ions. Multiply charged species (up to  $Cl^{5+}$  in chloroethylene) are formed; in all the halogen-containing ions, double-peaks with relative intensities consistent with the isotopic abundance ratios are observed. The mass spectrum for 2-chloroethylsilane is somewhat more complex, probably reflecting the larger number of dissociation channels available for this molecule. The parent ion is accompanied by dehydrogenation products of the parent molecule; other polyatomic fragments containing Si-H, C-Si, Cl-Si, and C-Cl bonds are also formed; multiply charged silicon ions (up to  $Si^{4+}$ ) can also be assigned. In the three systems, background signals due to oxygen, nitrogen, and particularly water are also present. In addition to the double structure due to the isotopic forms of the halogens, the peaks due to multiply charged atomic ions are split into two components. The characteristic doublet structure is exemplified by the  $C^{2+}$  peaks in the inset of Figure 1. The mass spectra of cyclopropane are dominated by the C-groups, including the parent molecule  $C_3H_n^+$ , in agreement with previous work.<sup>3,4</sup>

We note that our TOF spectra are likely to be free of any effects of clustering. We found, moreover, that enhancing the stagnation pressure up to  $10^5$  Pa with the addition of He did not affect significantly the mass spectra of the studied molecules.

The mass spectra change with laser intensity: generally the signal from the lower  $M/q$  (mass-to-charge ratio) ions increases at the expense of the higher  $M/q$  ions as the laser intensity is increased. Figure 2 shows a log-log dependence of the ion yield on laser intensity for Si and C ions produced by the dissociative ionization of 2-chloroethylsilane. A saturation of the process causes the slope to decrease with laser intensity as the onset for the appearance of the higher charge ions is reached. Figure 2 presents the results for both p- and s-polarizations.

The splitting of the multiply charged atomic ions is seen to increase with laser intensity. This splitting has been previously

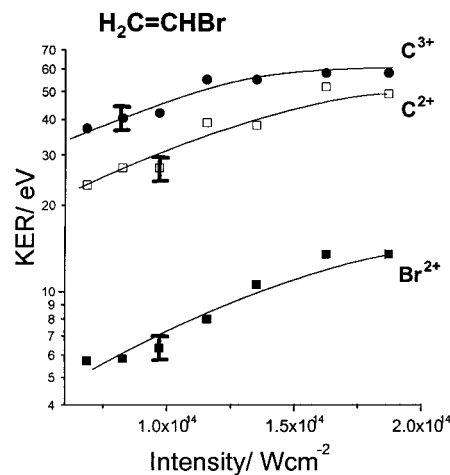


**Figure 3.** Maximum KER of C and Br atomic ions originated in the p-polarized, 800 nm 50 fs laser dissociative ionization of bromoethylene as a function of laser intensity. Differences in arrival times of the corresponding ions have been converted to kinetic energy (see text). Open squares  $C^{2+}$ , full squares  $C^{3+}$ , and open triangles  $Br^{2+}$ . Typical error bars are indicated in each plot. The lines are visual guides.

presented as evidence of a Coulomb explosion event<sup>8</sup> due to the existence of forward and backward turnaround time for ions ejected parallel and antiparallel to the polarization direction of the laser. Temporal peak separation,  $\Delta t$ , is related to the kinetic energy release (KER),  $E_{kin}$ , by<sup>18</sup>

$$E_{kin} = e^2 q^2 U^2 \Delta t^2 / 8M$$

where  $e$  is the elementary charge and  $U$  the collection electric field of the TOF spectrometer, about  $1300 \text{ V cm}^{-1}$ . The characteristic dependences of the KER on the laser intensity are shown in Figure 3 for the C and Br fragment ions produced by the dissociative ionization of bromoethylene. Similar behavior is found for the corresponding ions from chloroethylene and 2-chloroethylsilane. One can see that a higher laser intensity leads to the formation of ions that possess larger KER values; moreover, ions with a higher charge multiplicity exhibit a larger KER.

**3.2. Fragment Angular Distributions.** The angular distributions of the fragments were measured with the procedure reported in ref 7 by recording the TOF spectra as a function of different polarization angles over an interval of  $90^\circ$  with steps of  $2^\circ$ . The laser intensity was kept at about  $2 \times 10^{14} \text{ W cm}^{-2}$ . To facilitate the discussion of results, the data measured for a single quadrant were reflected and then used for the construction of the polar plots shown in Figures 4 and 5.

We found that ions produced by the dissociative ionization of chloroethylene and bromoethylene have similar angular distributions, Figure 4. The distributions of singly charged ions are nearly isotropic. In contrast, the distributions of multiply charged halogen and carbon ions exhibit a strong anisotropy, with a maximum at  $0^\circ$  (p-polarization). Thus, these fragments are preferentially ejected in the direction parallel (or antiparallel) to the laser electric field. The anisotropy is found to increase with the charge multiplicity. The same trend in the angular distributions is observed for Cl and Si ions produced by the dissociative ionization of 2-chloroethylsilane (i.e., singly charged ions having a nearly isotropic distribution and multiply charged ions an anisotropic one, with the anisotropy increasing with the charge multiplicity), Figure 5. However, the singly and multiply charged C ions behave differently: we found that s-polarization enhances their yield, cf. Figure 5.

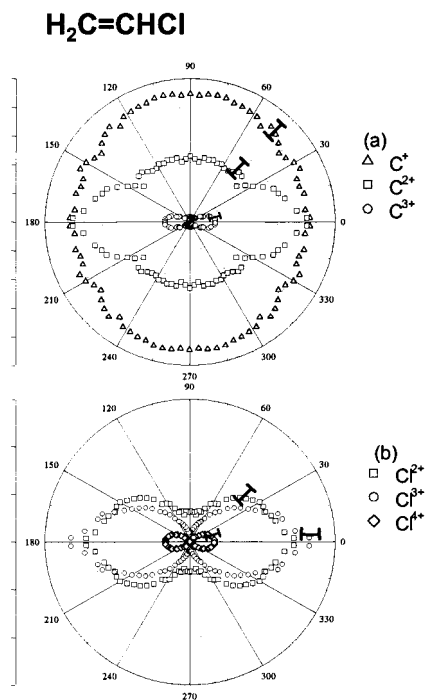


**Figure 4.** Polar plots of the angular distribution of (a) C and (b) Cl ions produced in the interaction of chloroethylene with 800 nm, 50 fs laser pulses at the intensity of  $1.7 \times 10^{14} \text{ W cm}^{-2}$ . Measurements were performed in the 0–90° quadrant and reflected in the other three for better visualization of results. The units of the polar coordinate indicated in the vertical scale have the same magnitude in both plots. Typical error bars are indicated in each plot.

The ions produced from cyclopropane show isotropic angular distributions except for the multiply charged C ions, which are markedly anisotropic along the p-polarization direction, and increasingly so with the increasing ion charge. The  $\text{C}^{2+}$  ions from chloroethylene, bromoethylene, and cyclopropane have an angular distribution that can be described by a superposition of an isotropic and a polarization-dependent component. The same type of angular distributions have been observed for atomic fragments from other polyatomic systems,<sup>7</sup> and have been attributed to two-pathways mechanism of forming the corresponding fragments.

To better understand the mechanisms of the ion fragment formation, we compared the fragment ion yields for orthogonal laser polarizations (p- and s-polarization) as a function of laser intensity. The results for Si and C ions produced from 2-chloroethenylsilane are shown in Figure 2. The ion yields are generally higher for p-polarized laser pulses; this is the case for the Si ions from 2-chloroethenylsilane (Figure 2a), all halogen ions, and two carbon ions produced by the dissociative ionization of chloro- and bromoethylene. For these ions, the ratio of the p- to s-polarization yield decreases with increasing laser intensity toward a constant value, equal to about 1 for singly charged ions and about 3 to 10 for multiply charged ions. This corresponds to a broadening of the angular distributions with increasing laser intensity. However, the ratio of the p- to s-polarization yield for the C ions produced from 2-chloroethenylsilane (Figure 2b) is <1 in the explored range of laser intensities.

#### 4. Discussion

Short pulse laser ionization and fragmentation can either proceed through a ladder-switching mechanism or by a direct, instantaneous Coulomb explosion of the parent molecule.<sup>33</sup> In

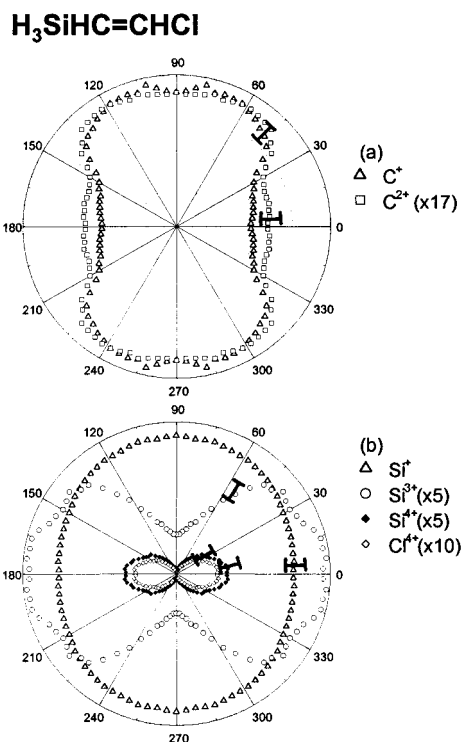


**Figure 5.** Polar plots of the angular distribution of (a) C and (b) Si and Cl ions produced in the interaction of 2-chloroethenylsilane with 800 nm, 50 fs laser pulses at the intensity of  $1.9 \times 10^{14} \text{ W cm}^{-2}$ . Ion signals have been multiplied by the indicated factors to ease the comparison. Measurements were performed in the 0–90° quadrant and reflected in the other three quadrants for better visualization of results. The units of the polar coordinate indicated in the vertical scale have the same magnitude in both plots. Typical error bars are indicated in each plot.

the case of the ladder switching mechanism, the singly or multiply ionized parent molecule dissociates into daughter molecular ions which dissociate further by unimolecular processes or give rise to smaller fragments through subsequent interaction with the laser field. In molecules similar to the ones studied here, internal conversion and fragmentation in electronically excited states of the parent proceeds within 30 fs.<sup>34,35</sup> Therefore in our case sequential fragmentation can take place within the duration of the laser pulse. For the direct Coulomb explosion mechanism, the ionization and dissociation are due to an instability, at some critical internuclear distance, of a highly charged parent species formed through multiphoton or tunnel ionization.<sup>36</sup>

The transition from the frequency-mediated coupling found in multiphoton processes to an electric field-mediated coupling, characteristic of field-induced ionization, is given by the value of the adiabaticity parameter, AP, introduced by Keldysh:<sup>37</sup>

$$AP = (E_i / (1.87 \times 10^{-13} I_0 \lambda^2))^{1/2}$$

Here  $E_i$  is the molecular ionization potential (in eV) in the absence of the laser field,  $I_0$  is the peak laser intensity (in  $\text{W cm}^{-2}$ ), and  $\lambda$  is the laser wavelength (in  $\mu\text{m}$ ). Values of  $AP > 1$  are indicative of a multiphoton ionization (MPI) mechanism; values  $< 1$  imply the participation of a field-ionization mechanism. At the highest laser intensity used in this work ( $2 \times 10^{14} \text{ W cm}^{-2}$ ), the value of AP is well below unity for all the molecules considered here. Levis et al.<sup>1</sup> proposed a structure-based model that predicts that the transition to the field ionization regime occurs at lower laser intensity than that

expected for an atomic species of the same ionization potential. Although field-induced effects should prevail in the interaction at the maximum laser intensity, parent ions can also be formed in the leading edge of the pulse and subsequently multiply ionized. These processes take place at lower intensities and involve species of higher ionization energy, implying substantially larger values of the AP. In addition, in the spatial regions outside of the Rayleigh range, the laser intensity reaches values considerably smaller than the maximum intensity. Hence both multiphoton ionization and field ionization are likely to participate in the dissociative ionization processes studied here.

If fragmentation favors charge symmetry,<sup>36</sup> then the observation of highly charged atomic fragments (charge multiplicity up to 5) would imply the existence of molecular transients that have twice the atomic charge. On the other hand, the characteristics of the observed peak splitting provide hints about the ionization and dissociation mechanisms.<sup>38</sup> The splitting of the peaks corresponding to multiply charged atomic ions is regarded as a signature of laser-induced Coulomb explosion; the splitting reveals different arrival times for the ions ejected forward and backward with respect to the TOF axis. Previous experiments with diatomic and polyatomic molecules have shown that, once a given channel is opened, the KER in Coulomb explosion processes is independent of laser intensity.<sup>33</sup> The increase of the KER with laser intensity observed in this work contradicts this mechanism. The latter behavior was also observed in multiply ionized fragments produced by ionization and dissociation of aromatic and single-bonded hydrocarbons with 50 fs laser pulses;<sup>4</sup> it was noted as indicative of a field-induced mechanism that produces ions with kinetic energies which increase with the electric field strength. This point will be further developed in a forthcoming paper.<sup>39</sup>

We now discuss the angular distributions of the fragment ions. The anisotropies observed in the angular distributions of the ion fragments have been explained in terms of various mechanisms. These include (a) a reorientation of the molecule by the interaction of the oscillating electric field of the laser with the anisotropic polarizability of the molecule;<sup>22</sup> (b) enhancement of the MPI rate of the parent molecule, or of the precursor fragments, when the electric vector of the linearly polarized light is parallel to the breaking bond of the molecule.<sup>14–16</sup> In our discussion we concentrate on these two mechanisms.

We have estimated the degree of the alignment induced by the anisotropic polarizability interaction for the halogenated ethylenes and cyclopropane parent molecules by following the quantum mechanical approach of Friedrich and Herschbach,<sup>22</sup> later extended for symmetric top molecules by Kim and Felker.<sup>40</sup> The nonresonant polarizability interaction induces a molecular alignment characterized by  $\langle\langle \cos^2 \theta \rangle\rangle$ , where  $\theta$  is the polar angle between the relevant axis of the molecule and the electric field vector. The ensemble average  $\langle\langle \cos^2 \theta \rangle\rangle$  of the expectation value of the alignment cosine depends on the dimensionless interaction parameter<sup>22</sup>  $\Delta\omega = 5 \times 10^{12} \Delta\alpha I_0/B$  and on the reduced rotational temperature  $\Gamma = kT/B$ , where  $I_0$  is the peak laser intensity in  $\text{W cm}^{-2}$ ,  $B$  the rotational constant in  $\text{cm}^{-1}$ ,  $T$  the rotational temperature, and  $\Delta\alpha$  is the polarizability anisotropy in  $\text{cm}^3$  (the difference between the polarizability components parallel and perpendicular to the relevant molecular axis). For the haloethylenes, considered here as prolate symmetric rotors, the relevant prolate axis is approximately the C–C bond. The relevant molecular axis in cyclopropane, an oblate symmetric rotor, is perpendicular to the molecular plane. We have calculated the components of the molecular polarizabilities using bond polarizabilities as reported in refs 41,42. Rotational

constants were taken from ref 43 or estimated using known bond distances and angles.<sup>41</sup>

The estimates of  $\langle\langle \cos^2 \theta \rangle\rangle$  for the maximum laser intensity of  $2 \times 10^{14} \text{ W cm}^{-2}$  and a rotational temperature  $T = 50 \text{ K}$  are near unity for chloroethylene, bromoethylene, and 2-chloroethenylsilane. In the case of cyclopropane, the anisotropic polarizability interaction would align the molecular plane along the electric field vector, and so there would be no preferred direction for the fragment ejection. However, the high degree of alignment cannot be achieved unless the laser interacts with the molecule adiabatically. This is the case when the laser pulse duration is greater than  $5h/(2\pi B)$  ( $h$  is Planck's constant).<sup>44</sup> In the case of the haloethylenes,  $h/(2\pi B)$  is on the order of a picosecond, way too long compared with the laser pulse duration of 50 fs. Therefore, in our case we expect no significant alignment of the molecular axis.

The measured ratios of the fragment ion yields for the two orthogonal laser polarizations at  $I = 5 \times 10^{12}$  to  $2 \times 10^{14} \text{ W cm}^{-2}$  provide an experimental evidence for a negligible role of the molecular axis alignment. The observed angular distributions of the ionic fragments for the halogenated ethylenes become more isotropic as the laser intensity increases. Just the opposite would be the case if molecular alignment were significant. Consequently, an alternative mechanism has to be invoked to explain the important features of the observed fragment angular distributions, such as the narrowing of the angular distributions for multiply charged ions and the propensity of multiply charged atomic ions to be ejected along the laser polarization. As discussed above, both field ionization and multiphoton ionization are likely to participate in the dissociative ionization of the molecules studied here. Recently the importance of ionic absorption has been discussed as a key factor in the formation of fragment ions during femtosecond laser excitation.<sup>45,46</sup> Molecular ions in suitable orientations can be promoted to excited states prior to further ionization or dissociation, through resonant absorption of laser photons. The rates of resonant photon absorption processes depend on the orientation of the molecular transition dipole moment with respect to the laser polarization. Resonant multiphoton absorption processes by parent ions select specific molecular orientations that lead to fragments with preferential orientations if bond breaking occurs in a time scale short compared to the overall rotation of the excited precursor. Thus, low-order multiphoton processes, responsible for the production of the parent ion, will take place in the low-intensity spatio-temporal part of the laser pulse, and will account for the observed isotropic angular distribution of these fragments. Higher order or Coulomb explosion processes, required to produce atomic fragments with higher charge multiplicity, are preceded by ultrafast geometrical deformation, possibly facilitated by the rapid elimination of some atoms,<sup>34,35</sup> and followed by anisotropic ejection of fragments representing the anisotropic formation of the parent molecular ion with respect to the laser polarization direction.<sup>19</sup> The propensity of the C ions from 2-chloroethenylsilane to be ejected perpendicular to the electric vector of the laser field (and to the Cl and Si multiply charged ions) can be related to the dissociation of multicharged parent molecules that have suffered an ultrafast modification of its initial geometry, so that the C–C bond is perpendicular to the C–Cl or C–Si bonds. For chloro- and bromoethylene, a fast opening of the C–C–X ( $X = \text{Cl, Br}$ ) angle to configure a linear geometry would account for the observed anisotropies.

Finally, we note that MPI of inner valence electrons<sup>9,47</sup> could be at least partly responsible for the observed anisotropies. This

mechanism implies a strong dependence of the MPI rate on the orientation of the molecule with respect to the laser field. If the MPI process is governed by the MPI rate of the atomic site having the highest degree of shielding from the atomic nuclear charge, then the angular distributions of the fragment ions would reflect the angular patterns of the atomic orbitals. That would explain the similar angular distributions of the halogen and carbon ions in chloro- and bromoethylene and would tie the different behavior of C ions from 2-chloroethenylsilane to the presence of the SiH<sub>3</sub> moiety attached to the C–C skeleton.

## 5. Conclusions

The angular distributions of multiply charged atomic ions produced by the dissociative ionization of chloroethylene, bromoethylene, and 2-chloroethenylsilane in an intense linearly polarized laser field (800 nm, 50 fs, 10<sup>14</sup> W/cm<sup>2</sup>) were found to exhibit marked anisotropies. These are likely to be due to the ultrafast geometric modifications of the parent molecule geometry during the short-pulse duration possibly aided by previous elimination of atomic moieties. The anisotropic fragment ejection represents the formation dependence of the ionization and dissociation rates on the orientation of the transition dipole moment of the parent or precursor fragment ions with respect to the direction of the linearly polarized laser field and the subsequent selection of orientation. The rate dependence can explain the main features of the measured angular distributions, such as the differences between the distributions of C<sup>n+</sup> from the haloethylenes, and the fact that angular distributions are narrower for ions with a higher charge multiplicity. The role of the molecular axis alignment is likely to be negligible because of the discrepancy between the long rotational period and the short pulse duration. The different observed anisotropies rule out the existence of a single precursor for all the fragments and firmly suggest the participation of parent or fragment precursors of different energies and degrees of ionization, some of them generated by resonant absorption with definite direction of transition moment. Multiply charged atomic ions are likely to be originated by Coulomb explosion of diatomic or triatomic ions, as higher size precursors would have to carry a very high charge and would hardly give rise to a defined direction of ejection. More work is in progress at different laser wavelengths and pulse durations to shed more light on the mechanisms involved.

**Acknowledgment.** The experiments were made possible thanks to financial support provided by the Ultraviolet Laser Facility, FoRTH-IESL under the Large Installations Plan of EU. This research has benefited from support from Project PB96-0844-C02-01 (DGICYT Spain). Dr. J. Pola is acknowledged for supplying the 2-chloroethenylsilane samples and Dr. M. Oujja for help with data analysis. M.C. is grateful for the hospitality received as a Visiting Scholar at the Chemical Laboratories, Harvard University. Special thanks go to Dr. B. Friedrich for discussions and critical reading of the manuscript.

## References and Notes

- Levis, R. J.; DeWitt, M. J. *J. Phys. Chem. A* **1999**, *103*, 6493.
- Ledingham, K. W. D.; Singhal, R. P.; Smith, D. J.; McCanny, T.; Graham, P.; Kilic, H. S.; Peng, W. X.; Langley, A. J.; Taday, P. F.; Kosmidis, C. *J. Phys. Chem. A* **1999**, *103*, 2952.
- Castillejo, M.; Couris, S.; Koudoumas, E.; Martín, M. *Chem. Phys. Lett.* **1998**, *289*, 303.
- Castillejo, M.; Couris, S.; Koudoumas, E.; Martín, M. *Chem. Phys. Lett.* **1999**, *308*, 373.
- Bhardwaj, V. R.; Rajgara, F. A.; Vijayalakshmi, K.; Kumarappan, V.; Mathur, D. *Phys. Rev. A* **1998**, *58*, 3449.
- Banergee, S.; Ravindra Kumar, G.; Mathur, D. *Phys. Rev. A* **1999**, *60*, R3369.
- Couris, S.; Koudoumas, E.; Leach, S.; Fotakis, C. *J. Phys. B* **1999**, *32*, L439.
- Hering, P.; Cornaggia, C. *Phys. Rev. A* **1999**, *59*, 2836.
- Talebpour, A.; Larochele, S.; Chin, S. L. *J. Phys. B* **1998**, *31*, 2769.
- Fraser, D.; Hutchinson, M. H. R.; Marangos, J. P.; Tisch, J. W. G.; Castillejo, M. *J. Phys. B* **1995**, *28*, L739.
- Hay, N.; Castillejo, M.; de Nalda, R.; Springate, E.; Mendham, K. J.; Marangos, J. P. *Phys. Rev. A* **2000**, *61*, 53810.
- Normand, D.; Lompré, L. A.; Cornaggia, C. *J. Phys. B* **1992**, *25*, L497.
- Bhardwaj, V. R.; Vijayalakshmi, K.; Mathur, D. *Phys. Rev. A* **1997**, *56*, 2455.
- Posthumus, J. H.; Plumridge, J.; Thomas, M. K.; Codling, K.; Frasiniski, L. J.; Langley, A. J.; Taday, P. F. *J. Phys. B* **1998**, *31*, L553.
- Ellert, C.; Corkum, P. B. *Phys. Rev. A* **1999**, *59*, R3172.
- Graham, P.; Ledingham, K. W. D.; McCanny, T.; Hankin, S. M.; Fang, X.; Smith, D. J.; Kosmidis, C.; Tzallas, P.; Langley, A. J.; Taday, P. F. *J. Phys. B* **1999**, *32*, 5577.
- Schmidt, M.; Dobosz, S.; Meynadir, P.; D'Oliveira, P.; Normand, D.; Charron, E.; Suzor-Weiner, A. *Phys. Rev. A* **1999**, *60*, 4706.
- Cornaggia, C.; Normand, D.; Morellec, J. *J. Phys. B* **1992**, *25*, L415.
- Iwamae, A.; Hishikawa, A.; Yamanouchi, K. *J. Phys. B* **2000**, *33*, 223.
- Frasinski, L. J.; Plumridge, J.; Posthumus, J. H.; Codling, K.; Taday, P. F.; Divall, E. J.; Langley, A. J. *Phys. Rev. Lett.* **2001**, *86*, 2541.
- Anderson, J. H.; Thomas, R. V.; Bryant, W. A.; Newell, W. R.; Taday, P. F.; Langley, A. J. *J. Phys. B* **1997**, *30*, 4499.
- Friedrich, B.; Herschbach, D. *Phys. Rev. Lett.* **1995**, *74*, 4623.
- Sakai, H.; Safvan, C. P.; Larsen, J. J.; Hilligsøe, K. M.; Hald, K.; Stapelfeldt, H. *J. Chem. Phys.* **1999**, *110*, 10235.
- Larsen, J. J.; Sakai, H.; Safvan, C. P.; Wendt-Larsen, I.; Stapelfeldt, H. *J. Chem. Phys.* **1999**, *111*, 7774.
- Sugita, A.; Mashino, M.; Kawasaki, M.; Matsumi, Y.; Gordon, R. J.; Bershon, R. *J. Chem. Phys.* **2000**, *112*, 2164.
- Blank, D. A.; Sun, W.; Suits, A. G.; Lee, Y. T.; North, S. W.; Hall, G. E. *J. Chem. Phys.* **1998**, *108*, 5414.
- Kay, R. D.; Raff, L. M. *J. Phys. Chem. A* **1997**, *101*, 1007.
- Castillejo, M.; de Nalda, R.; Oujja, M. *J. Photochem. Photobiol. A* **1997**, *110*, 107.
- Hay, N.; de Nalda, R.; Halfmann, T.; Mendham, K. J.; Mason, M. B.; Castillejo, M.; Marangos, J. P. *Phys. Rev. A* **2000**, *62*, 041803-1.
- Hansch, P.; Walker, M. A.; Van Woerkom, L. D. *Phys. Rev. A* **1996**, *54*, R2559.
- Talebpour, A.; Chien, C. Y.; Chin, S. L. *J. Phys. B* **1996**, *29*, L677.
- Pola, J.; Bastl, Z.; Subrt, J.; Abeyinghe, J. R.; Taylor, R. *J. Mater. Chem.* **1996**, *6*, 155. Kay, R. D.; Raff, L. M. *J. Phys. Chem. A* **1997**, *101*, 1007.
- Cornaggia, C.; Schmidt, M.; Normand, D. *Phys. Rev. A* **1995**, *51*, 1431.
- Farmanara, P.; Stert, V.; Radloff, W. *Chem. Phys. Lett.* **1998**, *288*, 518.
- Mestdagh, J. M.; Visticot, J. P.; Elhanine, M.; Soep, B. *J. Chem. Phys.* **2000**, *113*, 237.
- Smith, D. J.; Ledingham, K. W. D.; Singhal, R. P.; McCanny, T.; Graham, P.; Kilic, H. S.; Tzallas, P.; Kosmidis, C.; Langley, A. J.; Taday, P. F. *Rapid Commun. Mass Spectrom.* **1999**, *13*, 1366.
- Keldysh, L. V. *Sov. Phys. JETP* **1965**, *20*, 1307.
- Banergee, S.; Ravindra Kumar, G.; Mathur, D. *J. Phys. B* **1999**, *32*, 4277.
- Castillejo, M.; Couris, S.; Koudoumas, E.; Martín, M. *Chem. Phys. Lett.*, in press.
- Kim, W.; Felker, P. M. *J. Chem. Phys.* **1998**, *108*, 6763.
- Handbook of Chemistry and Physics*; CRC Press: Boca Raton, FL, 1999.
- Hirschfelder, J. D.; Curtiss, C. F.; Bird, R. B. *Molecular Theory of Gases and Liquids*; J. Wiley and Sons: New York, 1954.
- Herzberg, G. *Molecular Spectra and Molecular Structure III. Electronic Spectra of Polyatomic Molecules*; Van-Nostrand Reinhold: New York, 1966.
- Ortigozo, J.; Rodriguez, M.; Gupta, M.; Friedrich, B. *J. Chem. Phys.* **1999**, *110*, 3870.
- Fuss, W.; Schmid, W. E.; Trushin, S. A. *J. Chem. Phys.* **2000**, *112*, 8347.
- Harada, H.; Shimizu, S.; Yatsuhashi, T.; Sakabe, S.; Izawa, Y.; Nakashima, N. *Chem. Phys. Lett.* **2001**, *342*, 563.
- Talebpour, A.; Bandrauk, A. D.; Yang, J.; Chin, S. L. *Chem. Phys. Lett.* **1999**, *313*, 789.